ENGINEERING TRANSACTIONS • Engng. Trans. • 41, 1, 3–20, 1993
Polish Academy of Sciences • Institute of Fundamental Technological Research

APPLICATION OF THE CLASSICAL RAYLEIGH-RITZ METHOD IN DYNAMICS OF CIRCULAR ARCHES

B. OLSZOWSKI (KRAKÓW)

The paper deals with Rayleigh-Timoshenko and Bernoulli-Euler models of circular arches with extensible or inextensible axes clamped with free radial sliding at both ends. The general algebraic equation defining the eigenproblem has been derived from Hamilton's principle. Spectral properties of the models were analysed by means of the classical Rayleigh-Ritz approximation method. Eigenfrequencies as functions of the subtending angle of the arch are plotted and tabulated.

NOTATION

$U = \overline{U}/L$	radial displacement,
$W = \overline{W}/L$	tangential displacement,
$\Phi = \overline{\Phi}$	angular displacement,
$Q = L^2\overline{Q}/(EI)$	shear force,
$N = L^2\overline{N}/(EI)$	axial force,
$M = L\overline{M}/(EI)$	bending moment,
$p^2 = \mu\overline{A}L^4\omega^2/(EI)$	circular frequency,
$f = 4p/\pi^2$	comparative frequency,
$r = J/(\overline{A}L^2)$	moment of rotary inertia,
ξ	coordinate measured along the axis,
2α	subtending angle of the arch,

$\nu_1 = 1,\ \nu_2 = EI/(L^2EA),\ \nu_3 = EI/(L^2kGA).$

1. INTRODUCTION

Analysis of circular arches with hinged ends and constant length of the axis has revealed [6] a considerable complexity of their eigenspectra treated as functions of the angle α. Variation of this angle changes the positions of all the eigenfrequencies and their mutual distances. As a consequence, for some particular values of α, multiple or very close eigenfrequencies may appear. These facts manifest the existence of some behavioural singularities of the vibrating arches being at the same time not only quantitative but also qualitative in their nature [5/III]. Therefore, there seems to be a reasonable need to continue the analyses of the singularities being of interest from both the cognitive and the practical points of view. The latter, for instance, has the essential meaning when the eigenproblems have to be solved by means of approximation methods.

The aim of the present paper is to apply the classical Rayleigh-Ritz method to the solution of dynamical eigenproblems for three fundamental modeles of circular arches: 1) Rayleigh-Timoshenko (RT), 2) Bernoulli-Euler with extensible axis (BEe), and 3) – with inextensible axis (BEi). The essential advantage of this application arises directly from the use of global approximation technique, because it simply avoids the modelling defects (element locking and spurious modes) caused always by the local approximations commonly used in the FEM [1,2].

The numerical analysis of the eigenfrequencies was performed for arches clamped at both ends, with clamps allowing for frictionless radial sliding. Proper selection of the global Ritz approximation basis [3,4] yields, in this case of boundary conditions, accurate numerical results, i.e. not disturbed by any approximation errors. The eigenspectra were treated as functions of the angle 2α subtended by the arch. The results of computations enabled verification of previous outcomes obtained for circular rings and published in [5/I]. At the same time, a convenient reference point was set up for further analyses.

2. Formulation of eigenproblems

2.1. *Model* RT

Let us consider a circular arch with constant length $2L$ (Fig. 1) and the state of displacement described by three independent functions $\overline{w}(s,t)$, $\overline{u}(s,t)$ and $\varphi(s,t)$ [5/I]. The kinetic and potential energies of the vibrating arch are defined by the formulae

$$T = \frac{1}{2}\int_{-L}^{L}\left(\mu A\dot{\overline{w}}^2 + \mu A\dot{\overline{u}}^2 + \mu J\dot{\varphi}^2\right) ds,$$

$$U = \frac{1}{2}\int_{-L}^{L}\left[EI(\varphi')^2 + EA(\overline{w}' - \overline{u}/R)^2 + kGA(\overline{u}' + \overline{w}/R - \varphi)^2\right] ds.$$

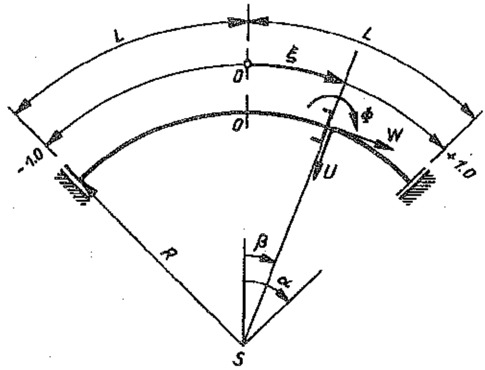

FIG. 1.

Confining further considerations to the stationary and harmonic vibration only, we assume that

$$\overline{w}(s,t) = \overline{W}(s)\sin(\omega t), \quad \overline{u}(s,t) = \overline{U}(s)\sin(\omega t), \quad \varphi(s,t) = \Phi(s)\sin(\omega t).$$

After introduction of some dimensionless quantities (see Notation) we obtain

$$T = \frac{1}{2}\frac{EI}{L}p^2\cos^2(\omega t)\int_{-1}^{1}\mathbf{R}^T(\xi)\boldsymbol{\rho}\mathbf{R}(\xi)\,d\xi, \qquad \boldsymbol{\rho} = \operatorname{diag}(1\ 1\ r),$$

$$U = \frac{1}{2}\frac{EI}{L}\sin^2(\omega t)\int_{-1}^{1}(\boldsymbol{\partial}\mathbf{R}(\xi))^T\boldsymbol{\sigma}(\boldsymbol{\partial}\mathbf{R}(\xi))\,d\xi, \qquad \boldsymbol{\sigma} = \operatorname{diag}(\sigma_1\ \sigma_2\ \sigma_3),$$

where

$$(2.1) \qquad \boldsymbol{\partial} = \begin{bmatrix} 0 & 0 & \partial \\ \partial & -\alpha & 0 \\ \alpha & \partial & -1 \end{bmatrix}, \qquad \partial \equiv d/dx, \qquad \mathbf{R}(\xi) = \begin{bmatrix} W(\xi) \\ U(\xi) \\ \Phi(\xi) \end{bmatrix}.$$

From Hamilton's principle

$$\delta H = \int_{t_0}^{t_1}(\delta T - \delta U)\,dt = 0,$$

after integration over the time interval $[t_0, t_1] \doteq [t, t + 2\pi/\omega]$ covering one period of vibration, it follows that

$$(2.2) \qquad \int_{-1}^{1}\Big[(\boldsymbol{\partial}\delta\mathbf{R}(\xi))^T\boldsymbol{\sigma}(\boldsymbol{\partial}\mathbf{R}(\xi)) - p^2\delta\mathbf{R}^T(\xi)\boldsymbol{\rho}\mathbf{R}(\xi)\Big] = 0.$$

Equation (2.2) sets up a basis for the numerical solution of the eigenproblem of a vibrating arch by means of an approximation method.

In what follows use will be made of the classical Rayleigh-Ritz method. Let us assume that

$$\mathbf{R}(\xi) = \mathbf{N}(\xi)\mathbf{q} = \begin{bmatrix} \mathbf{W}(\xi) & \mathbf{0} & \mathbf{0} \\ \mathbf{0} & \mathbf{U}(\xi) & \mathbf{0} \\ \mathbf{0} & \mathbf{0} & \mathbf{\Phi}(\xi) \end{bmatrix} \begin{bmatrix} \mathbf{a} \\ \mathbf{b} \\ \mathbf{c} \end{bmatrix}, \tag{2.3}$$

where

$$\begin{aligned} \mathbf{W}(\xi) &= [W_1(\xi),\, W_2(\xi),\, \ldots,\, W_n(\xi)], \\ \mathbf{U}(\xi) &= [U_1(\xi),\, U_2(\xi),\, \ldots,\, U_n(\xi)], \\ \mathbf{\Phi}(\xi) &= [\phi_1(\xi),\, \phi_2(\xi),\, \ldots,\, \phi_n(\xi)] \end{aligned}$$

represent the sets of admissible functions.

After substitution of Eqs. (2.1), (2.3) into Eq. (2.2) one obtains

$$\left\{ \int_{-1}^{1} \left[(\boldsymbol{\partial}\mathbf{N}(\xi)^T \boldsymbol{\sigma}(\boldsymbol{\partial}\mathbf{N}(\xi)) - p^2 \mathbf{N}^T(\xi)\boldsymbol{\rho}\mathbf{N}(\xi) \right] d\xi \right\} \mathbf{q} = \mathbf{0} \tag{2.4}$$

and finally

$$(\mathbf{S} - p^2\mathbf{B})\mathbf{q} = \mathbf{0}, \qquad \mathbf{S}^T = \mathbf{S}, \qquad \mathbf{B}^T = \mathbf{B}, \tag{2.5}$$

where

$$\mathbf{S} = \begin{bmatrix} \mathbf{S}^{aa} & \mathbf{S}^{ab} & \mathbf{S}^{ac} \\ \mathbf{S}^{ba} & \mathbf{S}^{bb} & \mathbf{S}^{bc} \\ \mathbf{S}^{ca} & \mathbf{S}^{cb} & \mathbf{S}^{cc} \end{bmatrix}, \qquad \mathbf{B} = \begin{bmatrix} \mathbf{B}^{aa} & \mathbf{0} & \mathbf{0} \\ \mathbf{0} & \mathbf{B}^{bb} & \mathbf{0} \\ \mathbf{0} & \mathbf{0} & \mathbf{B}^{cc} \end{bmatrix}, \qquad \mathbf{q} = \begin{bmatrix} \mathbf{a} \\ \mathbf{b} \\ \mathbf{c} \end{bmatrix},$$

$$\begin{aligned} \mathbf{S}^{aa} &= \sigma_2 <\mathbf{W}', \mathbf{W}'> + \alpha^2\sigma_3 <\mathbf{W}, \mathbf{W}>, \\ \mathbf{S}^{ab} &= -\alpha\sigma_2 <\mathbf{W}', \mathbf{U}> + \alpha\sigma_3 <\mathbf{W}, \mathbf{U}'>, \\ \mathbf{S}^{ac} &= -\alpha\sigma_3 <\mathbf{W}, \mathbf{\Phi}>, \\ \mathbf{S}^{bb} &= \alpha^2\sigma_2 <\mathbf{U}, \mathbf{U}> + \sigma_3 <\mathbf{U}', \mathbf{U}'>, \\ \mathbf{S}^{bc} &= -\sigma_3 <\mathbf{U}', \mathbf{\Phi}>, \\ \mathbf{S}^{cc} &= \sigma_1 <\mathbf{\Phi}', \mathbf{\Phi}'> + \sigma_3 <\mathbf{\Phi}, \mathbf{\Phi}>, \\ \mathbf{B}^{aa} &= <\mathbf{W}, \mathbf{W}>, \quad \mathbf{B}^{bb} = <\mathbf{U}, \mathbf{U}>, \quad \mathbf{B}^{cc} = r <\mathbf{\Phi}, \mathbf{\Phi}>, \end{aligned} \tag{2.6}$$

and from the definition

$$<\mathbf{F}, \mathbf{G}> = \int_{-1}^{1} \mathbf{F}^T(\xi)\mathbf{G}(\xi)\, d\xi.$$

2.2. *Model* BEe

In this case we neglect the rotary inertia of the cross-section ($J = 0$) and the shear deformation of the bar ($kGA = \infty$). A kinematic constraint imposed on its state of displacement has the form of the differential equation $\overline{u}' + \overline{w}/R - \varphi = 0$ [5/I]. In consequence, the energies T and U are now defined by the formulae

$$T = \frac{1}{2}\int_{-L}^{L} \left(m\overline{A}\dot{\overline{w}}^2 + m\overline{A}\dot{\overline{u}}^2\right) ds,$$

$$U = \frac{1}{2}\int_{-L}^{L} \left[EI(\overline{u}'' + \overline{w}'/R)^2 + EA(\overline{w}' - \overline{u}/R)\right] ds.$$

The reasoning analogous to the foregoing one leads us again to Eq. (2.5), but this time

$$\mathbf{R}(\xi) = \begin{bmatrix} W(\xi) \\ U(\xi) \end{bmatrix} = \mathbf{N}(\xi)\mathbf{q} = \begin{bmatrix} \mathbf{W}(\xi) & \mathbf{0} \\ \mathbf{0} & \mathbf{U}(\xi) \end{bmatrix} \begin{bmatrix} \mathbf{a} \\ \mathbf{b} \end{bmatrix},$$

$$\boldsymbol{\partial} = \begin{bmatrix} \alpha\partial & \partial^2 \\ \partial & -\alpha \end{bmatrix}, \qquad \boldsymbol{\sigma} = \begin{bmatrix} \sigma_1 & 0 \\ 0 & \sigma_2 \end{bmatrix}, \qquad \boldsymbol{\rho} = \mathbf{I},$$

$$\mathbf{S} = \begin{bmatrix} \mathbf{S}^{aa} & \mathbf{S}^{ab} \\ \mathbf{S}^{ba} & \mathbf{S}^{bb} \end{bmatrix}, \qquad \mathbf{B} = \begin{bmatrix} \mathbf{B}^{aa} & \mathbf{0} \\ \mathbf{0} & \mathbf{B}^{bb} \end{bmatrix}, \tag{2.7}$$

$$\mathbf{S}^{aa} = \left(\alpha^2\sigma_1 + \sigma_2\right) <\mathbf{W}', \mathbf{W}'>,$$

$$\mathbf{S}^{ab} = \alpha\sigma_1 <\mathbf{W}', \mathbf{U}''> - \alpha\sigma_2 <\mathbf{W}', \mathbf{U}>,$$

$$\mathbf{S}^{bb} = \sigma_1 <\mathbf{U}'', \mathbf{U}''> + \alpha^2\sigma_2 <\mathbf{U}, \mathbf{U}>,$$

$$\mathbf{B}^{aa} = <\mathbf{W}, \mathbf{W}>, \qquad \mathbf{B}^{bb} = <\mathbf{U}, \mathbf{U}>.$$

2.3. *Model* BEi

The constraint condition of axial inextensibility of the bar reads $\overline{w}' - \overline{u}/R = 0$, but it does not allow to eliminate any of the unknown functions from considerations. Both of them appear in the formula

$$T = \frac{1}{2}\int_{-L}^{L} \left(\mu\overline{A}\dot{\overline{w}}^2 + \mu\overline{A}\dot{\overline{u}}^2\right) ds,$$

and have to be treated equivalently.

In order to fulfil the constraint condition, we will handle the problem using the concept of Lagrange's multiplier. Let us use the modified function

$$U = \frac{1}{2}\int\limits_{-L}^{L} \left[EI(\overline{u}'' + \overline{w}'/R)^2 + \lambda(\overline{w}' - \overline{u}/R)\right] ds$$

containing an additional term with the unknown Lagrange's multiplier $\lambda(\xi) = N(\xi)$ being the axial force. This term may be interpreted as the work done by the axial force on the elongation of the axis.

Introduction of the dimensionless quantities leads to the following formulae:

$$\begin{aligned} T &= \frac{1}{2}\frac{EI}{L}p^2\cos^2(\omega t)\int\limits_{-1}^{1}(W^2 + U^2)\, d(\xi), \\ U &= \frac{1}{2}\frac{EI}{L}\sin^2(\omega t)\int\limits_{-1}^{1}\left[\sigma_1(U'' + \alpha W')^2 + \Lambda(W' - \alpha U)\right] d(\xi), \\ \Lambda &= \frac{\lambda L^2}{EI}. \end{aligned}$$

By means of Hamilton's principle we obtain the equation

$$\tag{2.8} \int\limits_{-1}^{1}\Big\{p^2(\delta W\cdot W + \delta U\cdot U) - \sigma_1(\delta U'' + \alpha\delta W')(U'' + \alpha W') - \frac{1}{2}\left[\delta\Lambda(W' - \alpha U) + (\delta W' - \alpha\delta U)\Lambda\right]\Big\}\, d(\xi) = 0$$

being the stationarity condition of the extended functional H. Making use of the approximations

$$W(\xi) = \mathbf{W}(\xi)\mathbf{a}, \qquad U(\xi) = \mathbf{U}(\xi)\mathbf{b}, \qquad \Lambda(\xi) = \mathbf{\Lambda}(\xi)\mathbf{c},$$

we may write Eq. (2.8) in the form (2.5) again, but with

$$\begin{aligned} \mathbf{S}^{aa} &= \sigma_1\alpha^2 < \mathbf{W}', \mathbf{W}' >, \\ \mathbf{S}^{ab} &= \sigma_1\alpha < \mathbf{W}', \mathbf{U}'' >, \\ \mathbf{S}^{ac} &= \frac{1}{2} < \mathbf{W}', \mathbf{\Lambda} >, \\ \mathbf{S}^{bb} &= \sigma_1 < \mathbf{U}'', \mathbf{U}'' >, \\ \mathbf{S}^{bc} &= -\frac{1}{2}\alpha < \mathbf{U}, \mathbf{\Lambda} >, \\ \mathbf{S}^{cc} &= \mathbf{0}, \\ \mathbf{B}^{aa} &= < \mathbf{W}, \mathbf{W} >, \quad \mathbf{B}^{bb} = < \mathbf{U}, \mathbf{U} >, \quad \mathbf{B}^{cc} = \mathbf{0}. \end{aligned}$$

The eigenproblem (2.5) is now of a saddle-point-type because, in addition to the displacement-type variables **a** and **b**, it contains also the force-type variables **c**. To handle the eigenproblem of BEi-model in the standard way, let us first perform such a "symmetrical" elimination of the redundant unknown **c**, which leads to a modified, pure displacement-type eigenproblem, with positive definite matrices **S** and **B** representing the elastic and inertial properties of the arch with the active kinematic constraint, i.e. with a completely inextensible axis. This procedure is shortly described in Sec. 3.3.

3. Numerical solutions

The eigenproblems were analysed for clamped arch segments, the clamps allowing for free radial sliding at both the ends (Fig. 1). This case may be of lesser importance from the purely practical point of view, nevertheless it deserves certain attention due to some theoretical aspects. This is mainly why, on the one hand, it enables us to verify the results already known for the unsupported circular rings [5/I] and, on the other hand, it creates a convenient reference point for further numerical analyses.

The eigenproblems were solved by means of the classical Rayleigh-Ritz method leading in the case of the boundary conditions considered to the accurate results. It is due to the fact that, just in this case, we can easily guess all the exact eigenmodes and use them as the elements of the classical Ritz approximation basis.

In order to simplify verification of the results and to improve the comparative analysis we have introduced the so-called comparative frequency $f = 4p/\pi^2$ [6]. The spectrum of these frequencies has, in the case of bending of a straight BEi-beam with hinged ends, a convenient representation as the sequence of squares of successive integers. This sequence may be easily found in tables and graphs representing the results of computations obtained for the BEe and BEi models.

3.1. Model RT

Computation of the whole eigenspectrum is possible only when two kinds of approximations are used. Taking into account the "visual predominance" of the radial displacement, we shall define them as symmetrical

$$\begin{aligned} W_k(\xi) &= \sin(k\pi\xi), \\ U_k(\xi) &= \cos(k\pi\xi), \\ \phi_k(\xi) &= \sin(k\pi\xi), \qquad k = 0, 1, 2, 3, \ldots, \end{aligned} \tag{3.1}$$

and antisymmetrical

$$\begin{aligned} W_k(\xi) &= \cos\left(k - \frac{1}{2}\right)\pi\xi, \\ U_k(\xi) &= \sin\left(k - \frac{1}{2}\right)\pi\xi, \\ \phi_k(\xi) &= \cos\left(k - \frac{1}{2}\right)\pi\xi, \qquad k = 1, 2, 3, \ldots . \end{aligned} \tag{3.2}$$

Substituting Eqs. (3.1), (3.2) into formulae (2.6) we obtain two distinct sequences of the algebraic equations (2.5) describing the successive but completely independent (3×3) eigenproblems:

for the case of symmetry

$$\left(\alpha^2\sigma_2 - p^2\right) b_0 = 0,$$

$$\begin{bmatrix} k^2\pi^2\sigma_2 + \alpha^2\sigma_3 - p^2 & -\alpha k\pi(\sigma_2 + \sigma_3) & -\alpha\sigma_3 \\ -\alpha k\pi(\sigma_2 + \sigma_3) & \alpha^2\sigma_2 + k^2\pi^2\sigma_3 - p^2 & k\pi\sigma_3 \\ -\alpha\sigma_3 & k\pi\sigma_3 & k^2\pi^2\sigma_1 + \sigma_3 - rp^2 \end{bmatrix} \tag{3.3}$$

$$\times \begin{bmatrix} a_k \\ b_k \\ c_k \end{bmatrix} = \mathbf{0}, \qquad k = 1, 2, 3, \ldots,$$

and for the case of antisymmetry

$$\begin{bmatrix} \left(k - \frac{1}{2}\right)^2 \pi^2\sigma_2 + \alpha^2\sigma_3 - p^2 & \alpha\left(k - \frac{1}{2}\right)\pi(\sigma_2 + \sigma_3) \\ \alpha\left(k - \frac{1}{2}\right)\pi(\sigma_2 + \sigma_3) & \alpha^2\sigma_2 + \left(k - \frac{1}{2}\right)^2 \pi^2\sigma_3 - p^2 \\ -\alpha\sigma_3 & -\left(k - \frac{1}{2}\right)\pi\sigma_3 \end{bmatrix} \tag{3.4}$$

$$\begin{matrix} -\alpha\sigma_3 \\ -\left(k - \frac{1}{2}\right)\pi\sigma_3 \\ \left(k - \frac{1}{2}\right)^2 \pi^2\sigma_1 + \sigma_3 - rp^2 \end{matrix} \Bigg] \begin{bmatrix} a_k \\ b_k \\ c_k \end{bmatrix} = \mathbf{0}, \qquad k = 1, 2, 3, \ldots .$$

In order to enable the comparisons between the present results and those obtained in [5/I] we have performed comparative calculations assuming for a semicircular arch

$$\alpha = \pi/2, \qquad r = 0.0048/\alpha^2, \qquad \nu_2 = r, \qquad \nu_3 = 0.01536/\alpha^2.$$

Table 1.

Pos	Results	$N=$	0	1	2	3	4	5	6	7
1	Ref. [1/I]	(1)			2.5798	6.9841	12.693	19.342	–	–
		(2)	14.434	20.363	32.225	45.604	59.480	73.572	–	–
		(3)	116.74	117.91	121.32	126.67	133.59	141.75	–	–
2	Symmetrical approximation Eq. (3.1)	(1)			2.5798		12.693		26.655	
		(2)	14.434		32.225		59.480		87.775	
		(3)			121.32		133.59		150.88	
3	Antisymmetrical approximation Eq. (3.2)	(1)				6.9841		19.342		34.429
		(2)		20.363		45.604		73.572		102.04
		(3)		117.91		126.67		141.75		160.77
4	Double antisymmetrical approximation Eq. (3.5)	(1)			2.5798		12.693		26.655	
		(2)			32.225		59.480		87.775	
		(3)	116.74		121.32		133.59		150.88	

The results are listed in Table 1 and we may notice that the frequency $p_{02} = 116.74$ is missing. This frequency may be obtained by means of the Rayleigh-Ritz method when we make use of the third kind of approximation with double antisymmetrical properties

$$\begin{aligned} W_k(\xi) &= \cos(k\pi\xi), \\ U_k(\xi) &= \sin(k\pi\xi), \\ \phi_k(\xi) &= \cos(k\pi\xi), \qquad k = 0, 1, 2, \ldots, \end{aligned} \tag{3.5}$$

leading to the following set of algebraic equations

$$\begin{bmatrix} \alpha^2\sigma_3 - p^2 & -\alpha\sigma_3 \\ -\alpha\sigma_3 & \sigma_3 - rp^2 \end{bmatrix} \begin{bmatrix} a_0 \\ b_0 \end{bmatrix} = \mathbf{0},$$

$$\begin{bmatrix} k^2\pi^2\sigma_2 + \alpha^2\sigma_3 - p^2 & k\pi\alpha(\sigma_2+\sigma_3) & -\alpha\sigma_3 \\ k\pi\alpha(\sigma_2+\sigma_3) & \alpha^2\sigma_2 + k^2\pi^2\sigma_3 - p^2 & -k\pi\sigma_3 \\ -\alpha\sigma_3 & -k\pi\sigma_3 & k^2\pi^2\sigma_1 + \sigma_3 - rp^2 \end{bmatrix} \begin{bmatrix} a_k \\ b_k \\ c_k \end{bmatrix} = \mathbf{0}, \tag{3.6}$$

$$k = 1, 2, 3, \ldots,$$

the results being listed in Table 1, pos.4. However, the approximation (3.5) does not fulfil the boundary conditions of the segment. The vibration with eigenfrequency $p_{02} = 116.74$ is therefore a unique eigenvibration of the circular unsupported ring and does not belong to the set of eigenvibrations of the clamped segment with radial sliding.

The results of eigenfrequency analysis performed for RT-segment are partially tabulated in Table 2 and are shown in Fig. 2 as the set of curves (f_k) representing the dependence: eigenspectrum versus angle α.

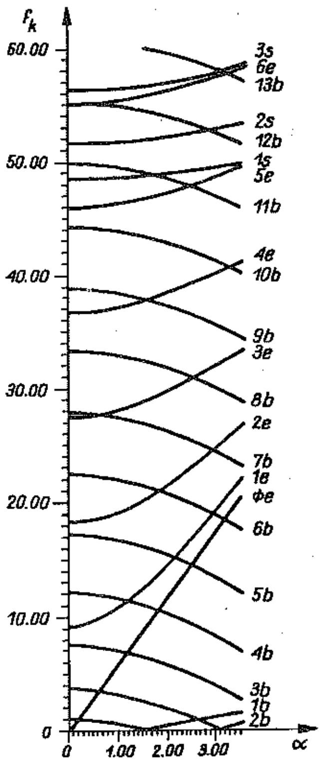

FIG. 2.

The eigenfrequencies f_k obtained on the basis of Eqs. (3.3), (3.4), form the triples is in Fig. 2 and Table 2 by symbols Lb, Le and Ls. Letter L is the number of vibration nodes common for each triple, and the second letter distinguishes the kind of predominating deformation of the vibrating bar, namely bending, extension and shearing. This notation corresponds to that applied in [5/1].

Table 2.

N	L	$a = 0.0$	L	$a = 0.5$	L	$a = 1.0$	L	$a = 1.5$	L	$a = 2.0$	L	$a = 2.5$	L	$a = 3.0$	L	$a = 3.5$
1	0e	0.000000	1b	0.835615	1b	0.489476	1b	0.062193	1b	0.374278	1b	0.794034	2b	0.232774	2b	0.588404
2	1b	0.976219	0e	2.924891	2b	3.129887	2b	2.543699	2b	1.831272	2b	1.047889	1b	1.191141	1b	1.566115
3	2b	3.662256	2b	3.522865	0e	5.849781	3b	6.431231	3b	5.655987	3b	4.749969	3b	3.751374	3b	2.691168
4	3b	7.547002	3b	7.415099	3b	7.032068	0e	8.774672	4b	10.326986	4b	9.402060	4b	8.353890	4b	7.210551
5	1e	9.188815	1e	9.641165	1e	10.871358	4b	11.096957	0e	11.699563	5b	14.541004	5b	13.496563	5b	12.339709
6	4b	12.166536	4b	12.042647	4b	11.678907	1e	12.636053	1e	14.737122	0e	14.624453	0e	17.549344	6b	17.771196
7	5b	17.208039	5b	17.091655	5b	16.748076	5b	16.192853	5b	15.448518	1e	17.048111	6b	18.911876	0e	20.474234
8	2e	18.377630	2e	18.607856	2e	19.270804	2e	20.298758	6b	20.808812	6b	19.931538	1e	19.492200	1e	22.021811
9	6b	22.483118	6b	22.373571	6b	22.049131	6b	21.521666	2e	21.613317	2e	23.144673	7b	24.462109	7b	23.350733
10	3e	27.566445	3e	27.720450	7b	27.472140	7b	26.971529	7b	26.291205	7b	25.448495	2e	24.873001	2e	26.646860
11	7b	27.882134	7b	27.778811	3e	28.169214	3e	28.877710	3e	29.799731	3e	30.887797	8b	30.073084	8b	28.996894
12	8b	33.341676	8b	33.244043	8b	32.953803	8b	32.478599	8b	31.830143	8b	31.022962	3e	32.098932	3e	33.396621
13	4e	36.755260	4e	36.870902	4e	37.209317	4e	37.747140	9b	37.388395	9b	36.616255	9b	35.703698	9b	34.665124
14	9b	38.825109	9b	38.732700	9b	38.457658	9b	38.006297	4e	38.451419	4e	39.285457	4e	40.213324	10b	40.330653
15	10b	44.311421	10b	44.223824	10b	43.962851	10b	43.533784	10b	42.944869	10b	42.206610	10b	41.330979	4e	41.202516
16	5e	45.944075	5e	46.036639	5e	46.308063	5e	46.740763	5e	47.309007	11b	47.782017	11b	46.942272	11b	45.979828
17	1s	48.350055	1s	48.380711	1s	48.472701	1s	48.626095	11b	48.487882	5e	47.982790	5e	48.731352	5e	49.525792
18	11b	49.788818	11b	49.705661	11b	49.457722	11b	49.049458	1s	48.841038	1s	49.117787	1s	49.456784	1s	49.858747
19	2s	51.553165	2s	51.589182	2s	51.697503	2s	51.878936	2s	52.134862	2s	52.467272	12b	52.530957	12b	51.605449
20	6e	55.132890	12b	55.171934	12b	54.936073	12b	54.547198	12b	54.011311	12b	53.336203	2s	52.878828	2s	53.372927
21	12b	55.250987	6e	55.210050	6e	55.436551	6e	55.798252	6e	56.273989	6e	56.838394	6e	57.464729	13b	57.204128
22	3s	56.287511	3s	56.329135	3s	56.454487	3s	56.665006	3s	56.963063	3s	57.351916	3s	57.835619	6e	58.127290
23	13b	60.694891	13b	60.619634	13b	60.394970	13b	60.024150	13b	59.512342	13b	58.866303	13b	58.093986	3s	58.418882

3.2. *Model* BEe

Similarly as in the RT-model, we shall use two kinds of approximations: symmetrical

$$(3.7)\qquad \begin{aligned} W_k(\xi) &= \sin(k\pi\xi), \\ U_k(\xi) &= \cos(k\pi\xi), \qquad k = 0, 1, 2, ..., \end{aligned}$$

and antisymmetrical

$$(3.8)\qquad \begin{aligned} W_k(\xi) &= \cos\left(k - \frac{1}{2}\right)\pi\xi, \\ U_k(\xi) &= \sin\left(k - \frac{1}{2}\right)\pi\xi, \qquad k = 1, 2, 3, \ldots . \end{aligned}$$

Substitution of Eqs. (3.7), (3.8) into Eq. (2.7) gives two corresponding sequences of the independent algebraic equations:

for symmetrical vibrations

$$\left(\alpha^2\sigma_2 - p^2\right) b_0 = 0,$$

$$(3.9)\qquad \begin{bmatrix} k^2\pi^2(\alpha^2\sigma_1 + \sigma_2) - p^2 & -\alpha k\pi(k^2\pi^2\sigma_1 + \sigma_2) \\ -\alpha k\pi(k^2\pi^2\sigma_1 + \sigma_2) & k^4\pi^4\sigma_1 + \sigma_2 - p^2 \end{bmatrix} \begin{bmatrix} a_k \\ b_k \end{bmatrix} = \mathbf{0}, \qquad k = 1, 2, 3, \ldots,$$

and for antisymmetrical vibrations

$$(3.10)\qquad \begin{bmatrix} \left(k - \frac{1}{2}\right)^2 \pi^2(\alpha^2\sigma_1 + \sigma_2) - p^2 & \alpha\left(k - \frac{1}{2}\right)\pi\left[\left(k - \frac{1}{2}\right)^2\pi^2\sigma_1 + \sigma_2\right] \\ \alpha\left(k - \frac{1}{2}\right)\pi\left[\left(k - \frac{1}{2}\right)^2\pi^2\sigma_1 + \sigma_2\right] & \left(k - \frac{1}{2}\right)^4\pi^4\sigma_1 + \alpha^2\sigma_2 - p^2 \end{bmatrix} \times \begin{bmatrix} a_k \\ b_k \end{bmatrix} = \mathbf{0}, \qquad k = 1, 2, 3, \ldots .$$

In Fig. 3 the results of complete eigenfrequency analysis are shown. Table 3 contains only the partial results, obtained for selected values of α.

Table 3.

N	L	$a = 0.0$	L	$a = 0.5$	L	$a = 1.0$	L	$a = 1.5$	L	$a = 2.0$	L	$a = 2.5$	L	$a = 3.0$	L	$a = 3.5$
1	0e	0.000000	1b	0.854640	1b	0.499254	1b	0.063349	1b	0.381530	1b	0.811698	2b	0.249069	2b	0.629837
2	1b	1.000000	0e	2.924891	2b	3.397729	2b	2.746962	2b	1.968500	2b	1.122839	1b	1.223198	1b	1.618008
3	2b	4.000000	2b	3.841072	0e	5.849781	3b	7.563854	3b	6.603736	3b	5.508836	3b	4.326563	3b	3.090855
4	3b	9.000000	3b	8.825988	3b	8.327672	0e	8.774672	0e	11.699563	4b	11.939216	4b	10.519855	4b	9.014957
5	1e	9.188815	1e	9.662309	1e	10.945789	1e	12.780339	4b	13.234791	0e	14.624453	0e	17.549344	5b	16.816105
6	4b	16.000000	4b	15.802765	4b	15.234670	4b	14.354945	1e	14.959601	1e	17.354628	5b	18.572382	0e	20.474234
7	2e	18.377630	2e	18.653249	2e	19.443091	2e	20.659959	5b	21.742581	5b	20.228556	1e	19.888819	1e	22.516114
8	5b	25.000000	5b	24.765546	5b	24.092624	5b	23.056023	2e	22.208706	2e	24.010066	2e	26.004710	6b	26.266149
9	3e	27.566445	3e	27.793483	3e	28.450418	3e	29.477091	3e	30.802103	6b	30.222464	6b	28.293094	2e	28.149490
10	6b	36.000000	6b	35.702125	6b	34.858995	6b	33.587285	6b	32.009582	3e	32.360987	3e	34.102746	3e	35.989337
11	4e	36.755260	4e	36.978343	4e	37.623908	4e	38.632496	4e	39.932536	4e	41.458501	7b	39.446134	7b	37.118010
12	5e	45.944075	5e	46.191057	5e	46.901551	7b	45.787695	7b	43.836459	7b	41.699245	4e	43.158107	4e	44.992330
13	7b	49.000000	7b	48.579401	7b	47.432439	5e	48.000728	5e	49.401684	5e	51.028070	8b	51.675586	8b	49.036641
14	6e	55.132890	6e	55.436417	6e	56.296502	6e	57.596465	8b	56.828120	8b	54.280339	5e	52.821332	5e	54.739285
15	8b	64.000000	8b	63.269495	8b	61.507275	8b	59.272444	6e	59.213706	6e	61.051633	6e	63.043065	6e	65.143302
16	7e	64.321704	7e	64.744445	7e	65.897832	7e	67.553284	7e	69.519509	7e	71.675991	7e	73.952649	7e	76.308594
17	8e	73.510519	8e	74.241545	8e	76.005327	8e	78.242762	8e	80.690730	8e	83.243197	8e	85.853677	8e	88.499389

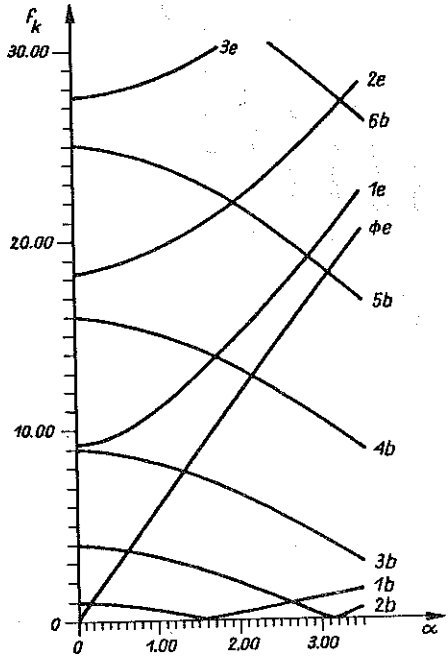

FIG. 3.

3.3. Model BEi

In this model we have to approximate three unknown functions, namely displacements $W(\xi)$, $U(\xi)$ and axial force $\Lambda(\xi)$, playing the role of Lagrange's multiplier. As in the foregoing cases, we make use of two kinds of approximations:

symmetrical

$$(3.11)\qquad \begin{aligned} W_k(\xi) &= \sin(k\pi\xi), \\ U_k(\xi) &= \cos(k\pi\xi), \\ \Lambda_k(\xi) &= \cos(k\pi\xi), \qquad k = 1, 2, 3, \ldots, \end{aligned}$$

and antisymmetrical

$$(3.12)\qquad \begin{aligned} W_k(\xi) &= \cos\left(k - \frac{1}{2}\right)\pi\xi, \\ U_k(\xi) &= \sin\left(k - \frac{1}{2}\right)\pi\xi, \\ \Lambda_k(\xi) &= \sin\left(k - \frac{1}{2}\right)\pi\xi, \qquad k = 1, 2, 3, \ldots \end{aligned}$$

leading to two corresponding sequences of the independent algebraic equations:

for the case of symmetry

$$\begin{bmatrix} k^2\pi^2\alpha^2\sigma_1 - p^2 & -k^3\pi^3\alpha\sigma_1 & \frac{1}{2}k\pi \\ -k^3\pi^3\alpha\sigma_1 & k^4\pi^4\sigma_1 - p^2 & -\frac{1}{2}\alpha \\ \frac{1}{2}k\pi & -\frac{1}{2}\alpha & 0 \end{bmatrix} \begin{bmatrix} a_k \\ b_k \\ c_k \end{bmatrix} = \mathbf{0}, \quad k = 1, 2, 3, \dots, \tag{3.13}$$

and for the case of antisymmetry

$$\begin{bmatrix} \left(k - \frac{1}{2}\right)^2 \pi^2\alpha^2\sigma_1 - p^2 & \left(k - \frac{1}{2}\right)^3 \pi^3\alpha\sigma_1 & -\frac{1}{2}\left(k - \frac{1}{2}\right)\pi \\ \left(k - \frac{1}{2}\right)^3 \pi^3\alpha\sigma_1 & \left(k - \frac{1}{2}\right)^4 \pi^4\sigma_1 - p^2 & -\frac{1}{2}\alpha \\ -\frac{1}{2}\left(k - \frac{1}{2}\right)\pi & -\frac{1}{2}\alpha & 0 \end{bmatrix} \times \begin{bmatrix} a_k \\ b_k \\ c_k \end{bmatrix} = \mathbf{0}, \qquad k = 1, 2, 3, \dots . \tag{3.14}$$

Solutions of both the eigenproblems (3.13), (3.14) were obtained by means of a "symmetrical" elimination of the redundant unknowns. Procedure of elimination is as follows: unknowns a_k and c_k are calculated from the third and the first equations, respectively, and then they are substituted into the second one. As a result, the equation is obtained describing the eigenproblem of the vibrating system with the imposed and active kinematic constraint.

Let us introduce a quantity

$$h = \begin{cases} k\pi & \text{for the case of symmetry,} \\ \left(k - \frac{1}{2}\right)\pi & \text{for the case of antisymmetry,} \quad k = 1, 2, 3, \dots \end{cases} \tag{3.15}$$

enabling us to solve both the eigenproblems (3.13), (3.14) simultaneously. From the third and the first equations we have

$$a_k = \pm(\alpha/h)b_k, \qquad c_k = (2\alpha/h^2)(h^4 - h^2\alpha^2 + p^2)b_k, \tag{3.16}$$

respectively, and from the second one, taking into account Eq. (3.15), we obtain

$$\left[h^6 - 2h^4\alpha^2 + h^2\alpha^4 - (h^2+\alpha^2)p^2\right] b_k = 0. \tag{3.17}$$

Equation (3.17) describes the constrained eigenproblem of the vibrating BEi-model and leads to the explicit formula for the eigenfrequencies (see Eq. (3.15))

$$p = \sqrt{(h^6 - 2h^4\alpha^2 + h^2\alpha^4)/(h^2+\alpha^2)} \, .$$

In the case when $\alpha = 0$, we obtain

$$p = h^2 = \begin{cases} (k\pi)^2 & \text{for symmetry,} \\ \left(k - \frac{1}{2}\right)^2 \pi^2 & \text{for antisymmetry,} \quad k=1,2,3,\ldots, \end{cases}$$

$$f = 4p/\pi^2 = \begin{cases} (2k)^2 & \text{for symmetry,} \\ (2k-1)^2 & \text{for antisymmetry,} \quad k=1,2,3. \end{cases}$$

The results concerning the eigenfrequencies are presented in Fig. 4 and in Table 4.

Table 4.

N	L	$a = 0.0$	L	$a = 0.5$	L	$a = 1.0$	L	$a = 1.5$
1	1b	1.000000	1b	0.856343	1b	0.501680	1b	0.063722
2	2b	4.000000	2b	3.850220	2b	3.425370	2b	2.786752
3	3b	9.000000	3b	8.849008	3b	8.407498	3b	7.707083
4	4b	16.000000	4b	15.848577	4b	15.400881	4b	14.675697
5	5b	25.000000	5b	24.848376	5b	24.397750	5b	23.660459
6	6b	36.000000	6b	35.848267	6b	35.396030	6b	34.651981

N	L	$a = 2.0$	L	$a = 2.5$	L	$a = 3.0$	L	$a = 3.5$
1	1b	0.383658	1b	0.815599	2b	0.254889	2b	0.644422
2	2b	2.006721	2b	1.147874	1b	1.228100	1b	1.623375
3	3b	6.792428	3b	5.712818	3b	4.515121	3b	3.239490
4	4b	13.701480	4b	12.512863	4b	11.147008	4b	9.640464
5	5b	22.655833	5b	21.408563	5b	19.946818	5b	18.300367
6	6b	33.629992	6b	32.348271	6b	30.828331	6b	29.093875

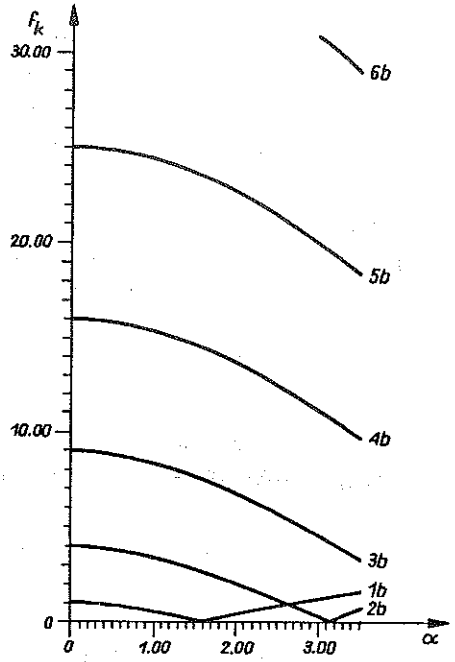

FIG. 4.

4. CONCLUSIONS

The models of circular arches clamped with free radial sliding at both ends represent the vibrating systems, the eigenfrequencies of which can be computed exactly by means of the classical Rayleigh-Ritz method. Using the exact eigenmodes as admissible functions we obtain, in the case of the RT model, a set of the separate triples of the homogeneous algebraic equations defining the separate (3×3) eigenproblems. This separation enables us to solve each eigenproblem independently, and to obtain always three exact eigenfrequencies corresponding to the exact eigenmodes denoted as Lb, Le and Ls (see Sec. 3), where L is a common number of vibration nodes. These eigenmodes are related to the three types of deformations with the characteristic predominance of bending, extension and shearing of the arch, respectively.

Two main advantages of application of the classical Rayleigh-Ritz method described in the present paper should be stressed. The first is that this method enables us to calculate the exact values of the eigenfrequencies owing to the special type of boudary conditions assumed. The second, and a more general advantage results from application of the global approximation technique enabling us to avoid completely all the numerical troubles, such as element locking and appearance of spurious modes, arising from the imperfections of the local approximations commonly used in the FEM [1,2].

The results described in the present paper confirm all the conclusions drawn in [5/1] and, therefore, set up a kind of a reliable "point of reference" for numerical analyses in the dynamics of circular arches.

References

1. D.G.Ashwell and R.H.Gallagher [Eds.], *Finite elements for thin shells and curved members*, Conf. on Finite Elements Applied to Thin Shells and Curved Members, University College, Cardiff 1974; J.Wiley and Sons Ltd., 1976.
2. K.C.Park and D.L.Flaggs, *A Fourier analysis of spurious mechanisms and locking in the finite element method*, Comp. Meth. Appl. Mech. Engng, **46**, 65–81, 1984.
3. L.Meirovitch, M.K.Kwak, *On the convergence of the classical Rayleigh-Ritz method and the finite element method*, AIAA J., **28**, 8, 1509–1516, 1990.
4. H.Baruh, S.S.K.Tadikonda, *Another look at admissible functions*, J. Sound Vibr., **132**, 1, 73–87, 1989.
5. B.Olszowski, *Free in-plane vibrations of unsupported circular rings. Part I. Natural frequencies* [in Polish], Engng. Trans., **37**, 3, 547–563, 1989; *Part II. Natural modes* [in Polish], Engng. Trans., **38**, 3–4, 185–202, 1990; *Part III. Free single frequency vibrations* [in Polish], Engng. Trans., **38**, 3–4, 203–219, 1990.
6. B.Olszowski, *Universal algorithm for generation of matrices used in dynamics of circular Timoshenko segments*, Engng. Trans., **40**, 2, 213–228, 1992.

KRAKÓW UNIVERSITY OF TECHNOLOGY.

Received November 20, 1991.